

Detection and attribution of trends in flood frequency under climate change in the Qilian Mountains, Northwest China

Xueliang Wang^{a,b,c,d}, Rensheng Chen^{a,*}, Hongyuan Li^{a,b}, Kailu Li^{a,b}, Junfeng Liu^a, Guohua Liu^{a,b}

^a Qilian Alpine Ecology and Hydrology Research Station, Key Laboratory of Ecohydrology of Inland River Basin, Northwest Institute of Eco-Environment and Resources, Chinese Academy of Sciences, Lanzhou 730000, China

^b University of Chinese Academy of Sciences, Beijing 100049, China

^c National Cryosphere Desert Data Center, Lanzhou 730000, China

^d Pingliang Hydrological Station of Gansu Province, Pingliang 744000, China

ARTICLE INFO

Keywords:

Trends
Flood frequency
Peaks-over-threshold
Climate change
Qilian mountains

ABSTRACT

Study region: The Qilian Mountains, Northwest China

Study focus: Trends in flood frequency and their driving factors must be analyzed to enable the effective management of water resources in the inland rivers originating in the Qilian mountains (QMs). Based on hydrological station datasets from 12 typical rivers with annual maximum peak discharge and peaks-over-threshold (POT) flood series for the period 1970–2019, the spatial and temporal variations of flooding in 12 rivers were detected using a linear regression estimator and Mann–Kendall trend tests.

New hydrological insights: The results indicate that the frequency of POT floods in 12 rivers during 1970–2019 showed an increasing trend at the 90% significance level, with an increasing trend for small floods and decreasing trends for medium and large floods. Flood levels varied from east to west across the region, with an overall decreasing trend in the east, an increase in small floods in the central rivers, and significant increases in both small and medium floods in the west. Both temperature and precipitation increased after 1987, and summer precipitation was a significantly increased; as a result, POT floods in most rivers increased after the 1980 s, and trends in flood frequency showed decreases in spring and autumn and an increase in summer. The main causes of the changes in flood frequency were found to be heavy rainfall, abnormal warming, and accelerated glacial melting.

1. Introduction

Climate change, dominated by global warming (IPCC, 2021), has become one of the most important environmental issues in the world today (Betts, 2011). Global climate change has led to temperature increases, extreme weather, frequent climatic events, and induces accelerated hydrological cycles at global and continental scales (Zhang et al., 2013; Ziegler et al., 2003). As such, the effects of climate change have aroused great concern and substantial interest from governments and researchers worldwide (Murray and Ebi, 2012). River floods are one of the most destructive types of natural disasters. Catastrophic flooding of different types (i.e., fluvial,

* Corresponding author.

E-mail address: crs2008@lzb.ac.cn (R. Chen).

<https://doi.org/10.1016/j.ejrh.2022.101153>

Received 1 May 2022; Received in revised form 19 June 2022; Accepted 21 June 2022

Available online 27 June 2022

2214-5818/© 2022 The Authors. Published by Elsevier B.V. This is an open access article under the CC BY-NC-ND license (<http://creativecommons.org/licenses/by-nc-nd/4.0/>).

pluvial, and coastal flooding) has gained public awareness and caused increasingly severe events over the past few decades, with an estimated average annual global cost of US\$104 billion (Desai et al., 2015). Extreme flooding events are projected to increase with ongoing climate change, urbanization, and economic growth (Hallegatte et al., 2013; Hirabayashi et al., 2013).

There are growing concerns over river floods due to changes in the magnitude, frequency, and trends of flooding events at catchment, continental, or global scales. Recent studies have indicated that climate change has both increased in northwestern Europe and decreased in medium and large catchments in southern Europe the frequency of river flooding events (Bloeschl et al., 2019; Bloeschl et al., 2017). Anthropogenic climate change was expected to increase flood risk through more frequent intense precipitation, increased catchment wetness and sea level rise (Wilby and Keenan, 2012). Studies have highlighted increasing changes in extreme flood events and future flood projections in the context of climate change, indicating that their frequency of occurrence is likely to increase in the future (Archfield et al., 2014; Chen et al., 2021; Murray and Ebi, 2012; Zadeh et al., 2020). Magnitude and frequency of floods across China has been projected to increase by varying degrees under 54 different warming scenarios (Gu et al., 2021; Kundzewicz et al., 2019a; Liang et al., 2019), and flood risk increased in several areas between 1961 and 2017 (Kundzewicz et al., 2019b). Yang et al. (2019) presented a characterization of flood hazards across China and indicated there has been a decrease in flood hazards in recent decades. Xiong et al. (2020) proposed that the magnitude of the annual maximum peak discharge in the Yangtze River has shown a decreasing trend since 1998, accompanied by periodic fluctuations in summer precipitation anomalies. Mao et al. (2012) found there is a link between extreme flooding and climate change that has occurred in arid and semi-arid regions of northwest China over the past 50 years, such as in typical watersheds in the Tianshan mountains, and that extreme flooding events are increasing in different regions in Xinjiang, with southern Xinjiang showing a significant increase. Zhang et al. (2016) studied flooding in the Tarim River basin, particularly in high-latitude rivers, where they found that floods are mainly attributable to intense precipitation and glacial melting, with rainstorm- and temperature-induced floods being dominant. The impact of climate change on river floods remains an important area of research because of the complexities surrounding changes in precipitation, underlying surface conditions, and the hydrological cycle.

The Qilian mountains (QMs) are the source and runoff formation area of inland rivers in the Hexi Corridor, which is a typical arid–semi-arid region in northwest China (Zhang et al., 2015). The inland rivers that originate in the QMs flow through the Hexi Corridor and disappear into the oases in the north. Nevertheless, mountainous areas located at high altitudes of QMs have special and typical flood generation mechanisms, where heavy rainfall and melting ice and snow water due to temperature increase are the main factors generating floods. Understanding the trends in the frequency changes of floods in the context of climate change is important for understanding the patterns of water resources changes, sustainable water resources management and environmental protection in northwest China (Chen et al., 2021). Although numerous studies have been conducted on hydrological factors in arid inland river basins in northwest China, these studies have focused mainly on the impact of climate change on runoff (Li et al., 2020; Ma et al., 2008; Wang and Qin, 2017), and few studies have focused on the correlation between climate change and flood-risk factors (Zhang et al., 2016). Most studies on flood-risk factors under the influence of climate change have not been sufficiently comprehensive. Moreover, the limited geographical source, environmental complexity, and length and quality of collated historical hydrological data for arid and

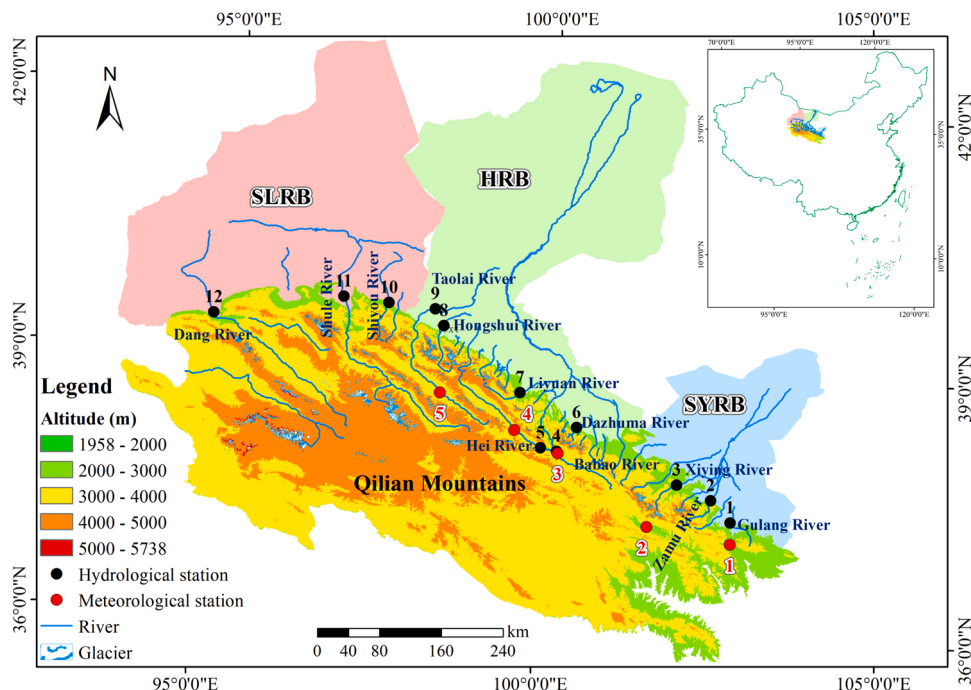


Fig. 1. Location of the study area.

semi-arid inland river basins have greatly limited our understanding of the impacts of climate change on flooding. As the temperature and precipitation in northwest China showed an increase after 1987 (Chen et al., 2015), the effects of such changes on river floods in the region remains unknown.

In this study, we comprehensively assessed the impact of the changing climate on flood frequency in the QMs using hydrological data and meteorological records for the period 1970–2019. The main objectives of our study were (1) to evaluate the spatial and temporal distributions of Peaks-Over-Threshold (POT) flood series, (2) to ascertain the trends of different levels and types of POT flood series at different temporal and regional scales, and (3) to explore the driving factors of changes in flood frequency, including the relationship between meteorological factors and flood characteristics.

2. Materials and methods

2.1. Study area

The QMs are located in the geographical boundary of about 93.4°–103.4°E and 35.8–40.0°N across the northeast Qinghai–Tibetan Plateau and northwest China, and extend > 800 km from northwest to southeast and > 200 km from south to north (Wang et al., 2019b). The Hexi Corridor inland region (92.4°–104.2°E, 37.3–42.3°N) is located in the north of the QM region, with a total area of 2.15×10^5 km². The QM region is composed of several parallel mountain belts and wide valleys orient northwest to southeast. The elevation of the region ranges from < 3000 to > 5000 m, with most peaks exceeding 4000 m (Wang et al., 2019b). Snow cover is typically present all year round on the mountains above 4000 m, and glaciers are more abundant in the west than in the east (Cao et al., 2014; Gao et al., 2011; Tian et al., 2014; Zhang et al., 2012). The climate shows substantial variation with altitude, and most precipitation events in high mountain areas are influenced by three main sources of water vapor; i.e., westerly flow, the East Asian monsoon, and the Tibetan Plateau monsoon (Zhang et al., 2008). The QMs are the runoff formation area and source of several major rivers, and the region has a mean annual rainfall of 301.9 mm (Wang et al., 2019a). In this study, we selected 12 rivers (Fig. 1) that originate from the QMs and terminate in the northern oasis of the Hexi Corridor. The rivers are distributed across three main basins from east to west; i.e., the Shiyang River basin (SYRB), the Hei River basin (HRB), and the Shule River basin (SLRB), respectively. The characteristics of these rivers are listed in Table 1.

2.2. Data

Twelve rivers originating from the QMs were selected for analysis of trends in flood frequency (Fig. 1, Table 1); these rivers were pristine and almost free from human influence. The dataset used in this paper was compiled from climate data and historical flood-discharge data. Climate data were obtained from the National Meteorological Centre of the China Meteorological Administration, and flood discharge data were collected from the Bureau of Hydrology and Water Resources of Gansu Province. General flood information is shown in Table 1, and information on the meteorological stations in the QMs is given in Table 2.

Our analysis was based on a series of observations of annual maximum peak discharge and POT flood series from 12 hydrological stations with continuous records over the period 1970–2019 (i.e., three stations in the SYRB, six stations in the HRB, and three stations in the SLRB). There are considerable variations in the spatial scales of the representative river basins, with a large percentage (~78%) of the stations representing small- and medium-sized river basins (drainage areas < 5000 km²; Table 1). The data have been subject to strict quality-control procedures to ensure data consistency and accuracy by following the procedure for hydrological data compilation of China, SL247–2012, and published in the previous hydrological yearbook.

Due to the complex topography, high altitude and inaccessibility of the Qilian Mountains, only five national meteorological stations are located in the high-altitude mountainous areas, while the rest of the meteorological stations are located in the pre-mountain and oasis plain areas. Data from five meteorological stations in the QMs were selected for this study. Daily precipitation and temperature data for the period 1970–2019 were used to calculate trends of changes.

Table 1
General information about the peak discharge stations/catchments.

River Basin	Code	River Name	Discharge Station					Periods of Records
			Station Name	Catchment Area (km ²)	Longitude	Latitude	Altitude (m)	
SYRB	1	Gulang	Gulang	878	102°52′	37°27′	2072	1970–2019
	2	Zamu	Zamusi	851	102°34′	37°42′	2010	1970–2019
	3	Xiyang	Jiutiaoling	1077	102°03′	37°52′	2270	1970–2019
HRB	4	Babao	Qilian	2452	100°14′	38°12′	2710	1970–2019
	5	Hei	Zhamashike	4986	99°59′	38°14′	2810	1970–2019
	6	Dazhuma	Wafangcheng	229	100°31′	38°29′	2440	1970–2019
	7	Liyuan	Sunan	1080	99°38′	38°51′	2264	1970–2019
	8	Hongshui	Xindi	1581	98°25′	39°34′	1880	1970–2019
	9	Taolai	Jiayuguan	7095	98°16′	39°45′	1695	1970–2019
SLRB	10	Shiyu	Yumen	656	97°33′	39°47′	2300	1970–2019
	11	Shule	Changmabao	10961	96°51′	39°49′	2080	1970–2019
	12	Danghe	Dangchengwan	14325	94°53′	39°30′	2176	1970–2019

Table 2
Basic information from meteorological stations in the QM.

Code	Meteorological station	Longitude (°)	Latitude (°)	Altitude (m)	Periods of records
1	Wushaoling	37.20	102.87	3045.10	1970–2019
2	Menyuan	37.38	101.62	2850.00	1970–2019
3	Qilian	38.18	100.25	2787.40	1970–2019
4	Yeniugou	38.42	99.58	3320.00	1970–2019
5	Tuole	38.80	98.42	3367.00	1970–2019

2.3. Methods

2.3.1. Standardization

To completely explore the effects of meteorological variables on flood frequency, 12 temperature and precipitation indices were defined (Table 3). Meteorological variables were standardised as follows, to capture changes in temperature and precipitation:

$$MI = \frac{MI - Mean(MI)}{Sd(MI)} \tag{1}$$

where *MI* is the meteorological indices for the year; *Mean(MI)* is the mean value of the meteorological indices; and *Sd(MI)* denotes the standard deviation of the meteorological indices. *MI* > 0 means that the meteorological indices are higher than the mean value and show an increasing trend, and vice versa.

2.3.2. Test methods for trend analysis

Tests to detect significant trends in hydro-meteorological time series are based on parametric or non-parametric methods. The linear regression estimator (LR estimator) is the most frequently applied method for trend analysis (Li et al., 2008). The Mann–Kendall (M–K) trend test (Kendall, 1975; Mann, 1945) is also recommended by the World Meteorological Organization and is extensively adopted to identify trends in hydrometeorological variables (Gocic and Trajkovic, 2013; Hamed, 2008; Sang et al., 2014; Yang et al., 2022). In this study, we employed the LR estimator and M–K trend test to explore trends in flooding and climate variables.

The M–K trend test is calculated as follows:

$$S = \sum_{i=1}^{n-1} \sum_{j=i+1}^n \text{sgn}(x(j) - x(i)) \tag{2}$$

with

$$\text{sgn}(x(j) - x(i)) = \begin{cases} 1 & \text{if } x(j) - x(i) > 0 \\ 0 & \text{if } x(j) - x(i) = 0 \\ -1 & \text{if } x(j) - x(i) < 0 \end{cases} \tag{3}$$

A positive (negative) value of *S* represents an increasing (decreasing) trend. When *n* > 8, the statistic *S* is almost distributed normally, and its mean *E(S)* and variance *Var(S)* are determined as follows.

$$E(S) = 0 \tag{4}$$

$$\text{Var}(S) = \frac{1}{18} \left[n(n-1)(2n+5) - \sum_{i=1}^m t_i(t_i-1)(2t_i+5) \right] \tag{5}$$

Table 3
Precipitation and temperature indices used in this study.

Abbreviation	Meteorological indices	Unit
AP	Annual precipitation	mm
AMDP	Annual maximum daily precipitation	mm
NPD	Number of precipitation days	d
P1	Number of precipitation days when Pre. ≥ 1 mm	d
P5	Number of precipitation days when Pre. ≥ 5 mm	d
P10	Number of precipitation days when Pre. ≥ 10 mm	d
PII	Precipitation intensity index	mm/d
AT	Average temperature per year	°C
TXX	Annual maximum value of daily maximum temperature	°C
TXN	Annual minimum value of daily maximum temperature	°C
TNX	Annual maximum value of daily minimum temperature	°C
TNN	Annual minimum value of daily minimum temperature	°C

where n is the number of data points; m is the number of tied groups; and t_i is the number of data in the tied group. The standardised normal test statistic Z is computed as follows:

$$Z = \begin{cases} \frac{S - 1}{\sqrt{\text{Var}(S)}} & \text{if } S > 0 \\ 0 & \text{if } S = 0 \\ \frac{S + 1}{\sqrt{\text{Var}(S)}} & \text{if } S < 0 \end{cases} \quad (6)$$

The null hypothesis (i.e., no significant trend in hydrometeorological time series) is rejected if the absolute value of Z is greater than the theoretical value $Z_{1-\alpha/2}$, where α is the statistical significance level. All trend results in this study were evaluated at significance levels of 90%, 95%, and 99%.

2.3.3. Calculation of flood return period

The common methods for flood return period calculation include Generalized Extreme Value (GEV) distribution (Smith et al., 2018; Yang et al., 2019), Pearson type III distribution (Milly et al., 2002; Yin et al., 2015) and log-logistic distribution (Shao et al., 2004), etc. The POT flood series in the arid and semi-arid regions of northwest China under climate change are non-stationary in the past decades. Based on theoretical and practical considerations, the GEV distribution is applicable and accurate for the calculation of hydrological extremes, so after the goodness-of-fit test for the flood extremes series, the GEV distribution is chosen to calculate the flood return period.

2.3.4. Frequency analysis of POT flood series

The flood samples of the POT model obey Generalized Pareto distribution (Durocher et al., 2018; Katz et al., 2002). In order to make the assumption of independence of the extracted flood peaks acceptable, the de-clustering method proposed by Lang et al. (1999) was used, while considering the POT sampling method that has been applied in arid and semi-arid regions of northwest China (Jiang et al.,

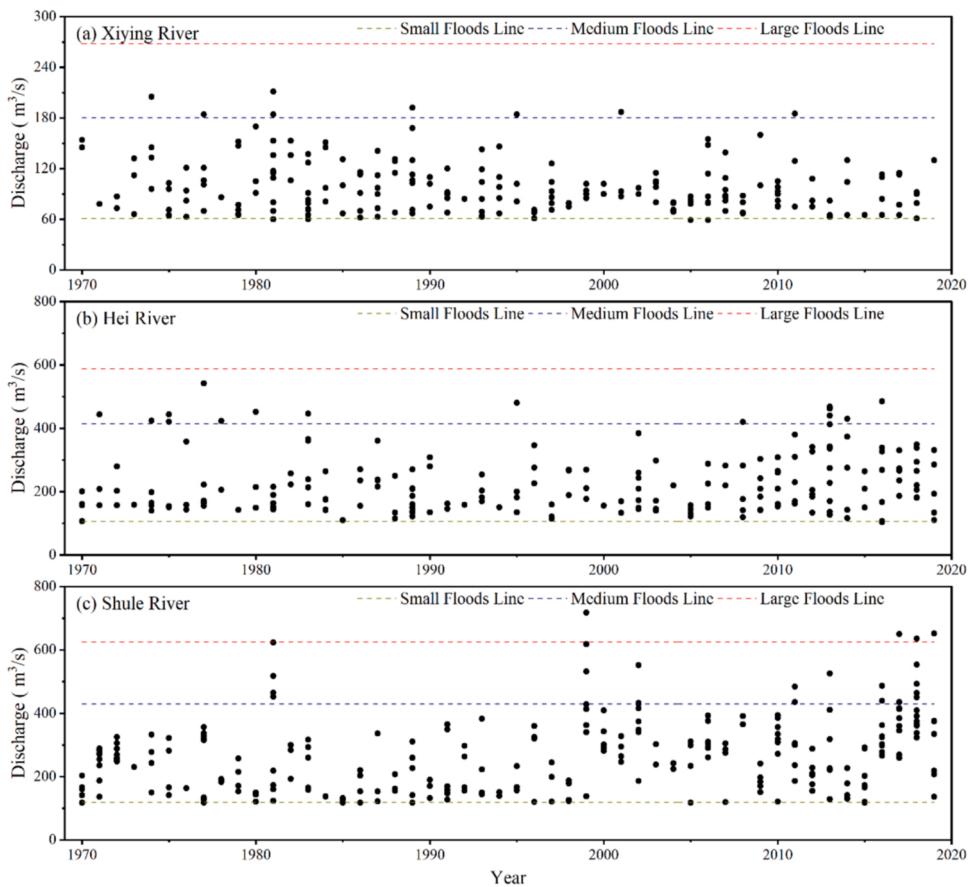


Fig. 2. Temporal variation of the flood frequency series. (a) Jiutiaoling hydrological station of Xiying River, (b) Zhamashike hydrological station of Hei River, (c) Changmabao hydrological station of Shule River. The dashed lines indicate the thresholds for small, medium and large floods.

2021; Zhang et al., 2016). In this study, all extracted peaks respect the following two conditions in terms of the interarrival time D and the intermediate discharge Q_{min} :

$$\left\{ \begin{array}{l} D > 5 + \log(A) \\ Q_{min} < \frac{3}{4} \min(Q_1, Q_2) \end{array} \right\} \quad (7)$$

where D denotes the flood duration between two successive peaks; A denotes the catchment area in km^2 ; and Q_{min} denotes the minimum discharge between two successive peaks Q_1 and Q_2 in m^3/s , respectively.

According to the Chinese hydrological information and forecasting specification (GB/T 22482–2008), flood levels are classified as follows: small flood (return period < 5 years); medium flood (return period = 5–20 years); and large flood (return period > 20 years). However, for inland rivers in arid and semi-arid regions, the number of floods per year was less and the magnitude of floods was much smaller compared to those occurring in large rivers in humid regions. In this study, in order to comprehensively detect frequency trends for different flood levels in 12 rivers originating in QMs under climate change, floods with return periods ≥ 1 years were selected as POT floods. To investigate flood frequency, correlation analysis of linear trend was also conducted to estimate the regional trends for the 12 studied rivers.

3. Results

3.1. The threshold value for POT sampling method

Floods with return periods ≥ 1 years were identified as POT floods, and the GEV distribution was used to calculate the return periods of the POT flood series for 12 rivers. The threshold determination of the POT sampling method will vary with the selection of different flood return periods. In the case of the Xiyang River in the east, the Hei River in the central and the Shule River in the west, for example, the flood peak discharge for a return period of 1 years were $60.8 \text{ m}^3/\text{s}$, $105.5 \text{ m}^3/\text{s}$ and $118.4 \text{ m}^3/\text{s}$, and the flood peak discharge increased as the return period increased, e.g., the flood peak discharge corresponding to a return period of 20 years were $268.1 \text{ m}^3/\text{s}$, $487.5 \text{ m}^3/\text{s}$ and $625.8 \text{ m}^3/\text{s}$, however, the POT floods events decreased and the temporal variation of the flood frequency series are shown in Fig. 2. According to the same evaluation method, the threshold values of POT floods for the corresponding hydrological stations of the 12 rivers are shown in Table 4.

3.2. Frequency trends for different flood levels

The results of temporal trend analysis of the different POT number of events (frequency) series using the LR estimator and M–K trend test are presented in Fig. 3. Significant increasing and decreasing trends in the frequency of POT flood series were found to have occurred in the study period, with 90%, 95%, and 99% significance levels. Specifically, an increase occurred in the frequency of total floods, with a significance level of 90%; this comprised an increase in the frequency of small floods and a decrease in the frequency of medium floods at the 95% significance level, whereas an insignificant change in the frequency of large floods.

Three main phases can be identified in the trends of total floods since 1970: from 1970 to 1987 there was a slight increase in flood frequency; from 1988 to 2009 there was a decrease in flood frequency; and after 2010 there was an increase in flood frequency. The trends for small and medium floods are similar to those for all flood classifications combined, whereas the trend for large floods is slightly different, with a decrease in flood frequency from 5.0 times/10 years during 1970–1987–3.75 times/10 years during 1988–2019.

Table 4

Threshold values of POT floods for the corresponding hydrological stations of the 12 rivers.

River Basin	Code	River Name	Discharge Station	
			Station Name	threshold values (m^3/s)
SYRB	1	Gulang	Gulang	5.0
	2	Zamu	Zamusi	49.6
	3	Xiyang	Jiutiaoling	60.8
HRB	4	Babao	Qilian	65.8
	5	Hei	Zhamashike	105.5
	6	Dazhuma	Wafangcheng	17.1
	7	Liyuan	Sunan	45.3
	8	Hongshui	Xindi	66.2
	9	Taolai	Jiayuguan	75.8
SLRB	10	Shiyou	Yumen	9.8
	11	Shule	Changmabao	118.4
	12	Danghe	Dangchengwan	32.6

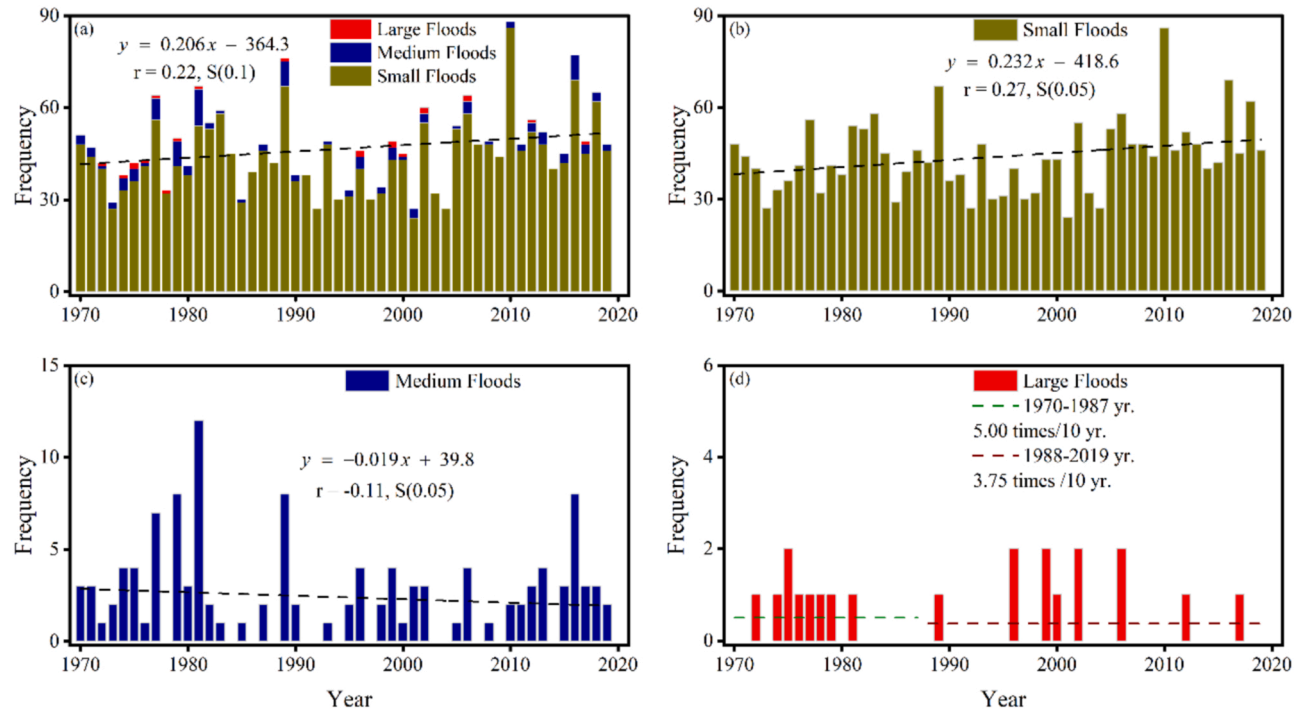


Fig. 3. Trends of flood frequency for 12 representative rivers in the QM region, northwest China. (a)–(d) Total, small, medium, and large floods, respectively. M–K trend tests for the various frequency series detected trends at the 90%, 95%, and 99% significance levels. S means statistically significant at the significance level shown in parentheses.

3.3. Frequency trends for different flood types

The results of the flood-type trend analysis and the percentage of each flood type are shown in Fig. 4 for the 12 studied rivers. Spring, summer, and autumn floods account for 15.4%, 79.7%, and 4.9% of the total floods, respectively. Spring and autumn floods showed decreasing frequency trends with significance levels of 99% and 95%, whereas summer floods exhibited an increasing frequency trend with a significance level of 99%. Spring floods showed an increasing frequency trend from 1970, a decreasing frequency trend after 1990, an increasing trend after 2000 followed by another decreasing frequency trend after 2010. Summer floods exhibited a continuously fluctuating increasing frequency trend from 1970 to 2019. In contrast, autumn floods showed a decreasing frequency trend from 1970 to 1985, and increasing frequency trend until approximately 1995, and then a fluctuating decreasing frequency trend until 2019.

3.4. Decadal trends in flood levels and types

Fig. 5 shows that the flood contains flood-abundant, normal, and dry years. In terms of flood size, small floods showed the least variation, with an increasing–decreasing–increasing trend from the 1970 s to the 2010 s. The medium floods showed a decreasing trend from the 1970 s to the 2000 s and an increasing trend after 2010. The large floods exhibited a decreasing trend from the 1970 s to the 1980 s, an increasing trend from the 1990 s to the 2000 s, and a further decreasing trend after 2010. The large floods showed the greatest variability, with a rate of variation of ~90% in the 1970 s and ~about 50% in the 1980 s and 2010 s

In terms of proportional analysis of flood types, spring floods increased from the 1970 s to the 1980 s and decreased from the 1990 s to the 2010 s. Summer floods showed the least variation, with a general increase overall from the 1970 s to the 2010 s. Autumn floods exhibited the greatest variation, decreasing from the 1970 s to the 2010 s, with a rate of variation of ~120% in the 1970 s and ~80% in the 2010 s

3.5. Regional trends in frequencies of various flood levels and types

The frequency trends for flood levels for the three main basins and a comparative analysis of regional variations in different flood levels are shown in Fig. 6. The changing climate led to both increasing and decreasing frequency trends in flood levels in the QM region from 1970 to 2019. In the SYRB, the frequency trends for small and large floods were nonsignificant, whereas medium floods exhibited a decreasing frequency trend with a significance level of 99%. In the HRB, small floods exhibited an increasing frequency trend with a significance level of 95%, but no significant frequency trends in medium or large floods were observed. In contrast to the SYRB and HRB, small and medium floods in the SLRB showed an increasing frequency trend with significance levels of 95% and 99%, respectively; no significant frequency trend was observed for large floods. Although various increasing and decreasing frequency trends were observed for small and medium floods in the three main basins, no significant frequency trends were observed for large floods.

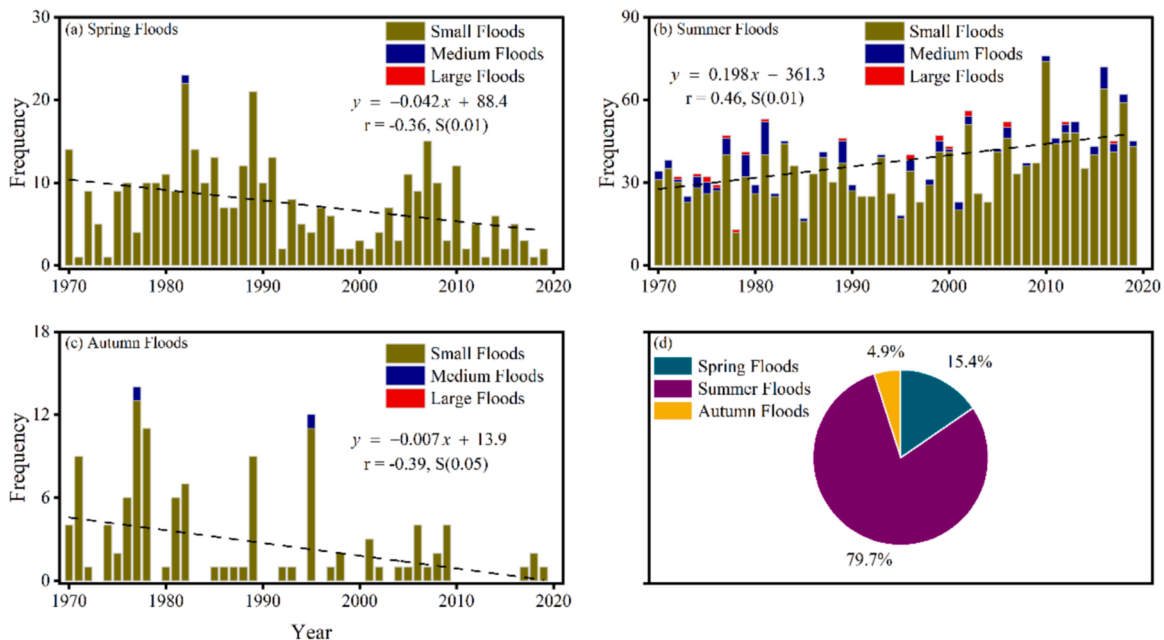


Fig. 4. Trends in flood frequency for 12 representative rivers in the QM region, northwest China. (a)–(d) Spring, summer, and autumn floods and percentages of different flood types, respectively. M–K trend tests for the various frequency series-detected trends at the 90%, 95%, and 99% significance levels. S means statistically significant at the significance level shown in parentheses.

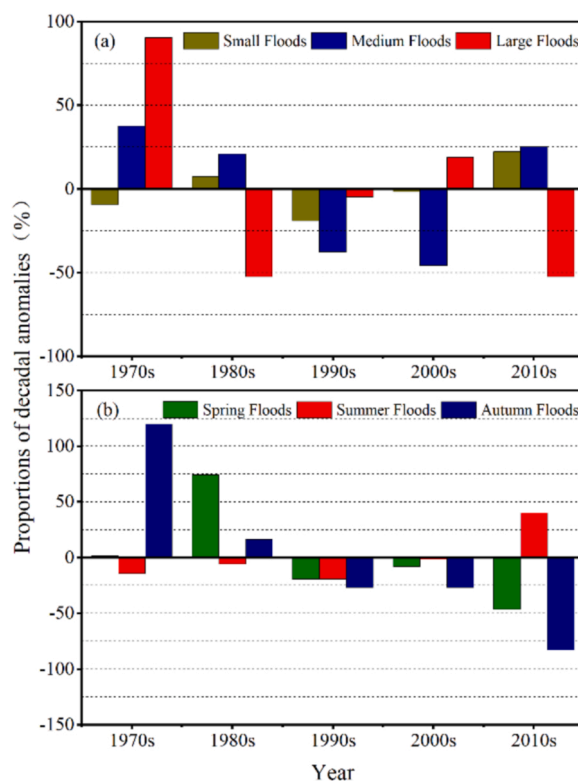


Fig. 5. Proportions of decadal anomalies in the POT flood series for 12 representative rivers in the QM region. (a) Proportions of small, medium, and large floods. (b) Proportions of spring, summer, and autumn floods.

Comparing the frequency of large floods before and after 1987, the frequency of large floods per decade was slightly increased in SLRB, while slightly decreased in SYRB and HRB.

The trends in flood frequency for the various flood types in the three studied basins are shown in Fig. 7. Variations were observed in the frequency of spring, summer, and autumn floods in the SYRB, HRB, and SLRB from 1970 to 2019. There were overall decreasing frequency trends for spring and autumn floods, with significance levels of 90% and 95% for the SYRB, 99% and 95% for the HRB, and overall decreasing frequency trends for both spring and autumn floods for the SLRB, with significance levels of 90%. Summer floods showed some variation, with a nonsignificant frequency trend in the SYRB and increasing frequency trends in the HRB and SLRB, both at a significance level of 99%.

4. Discussion

4.1. Possible attribution of flood frequency trends

The observed changes in flood frequency indicate that flooding showed significant variation from east to west in the QMs over the study period, as shown in Figs. 3–7. Changes in flood discharge since 1970 have been shown to be related to climate change in arid and semi-arid areas of northwest China (Mao et al., 2012; Wang and Qin, 2017). The climate is changing from warm–dry to warm–wet in this region (Shi et al., 2003), and a warmer climate may lead to high temperatures and heavy rainfall, and glacial melting may cause changes in flooding (Cao et al., 2014; Gao et al., 2011; Tian et al., 2014; Zhang et al., 2012). Chen et al. (2015) also found an increasing trend of temperature and precipitation in the arid northwest in the last 50 years, with precipitation at a relatively stable stage from 1960 to 1986, while it began to increase sharply after 1987, and it is noteworthy that the increasing trend slowed down from 2000 to 2015. To better understand the meteorological factors affecting changes in flood frequency, temperature and precipitation data from five meteorological stations were analysed by defining 12 temperature and precipitation indices (Figs. 8 and 9). The results of the analysis of data from the five stations indicate an increasing trend in temperature and precipitation from 1970 to 2019 (Figs. 8 and 9). Generally, the generation of floods is influenced by factors such as temperature, precipitation, and topography, but in the high–altitude areas of the QMs, precipitation is the dominant factor as the main cause of flood variability.

Under the influence of temperature and precipitation evolution from 1970 to 2019, variations in increasing or decreasing flood frequency trends were observed for the various flood levels and types in the SYRB, HRB, and SLRB (Figs. 3–7). According to Fig. 10, AP, P1 and P5 were counted for five weather stations in three sub-basins, and the results showed that AP was increasing trend in the whole region, and the increasing trend was more significant in the central and western than in the eastern region. P1 and P5 also showed a

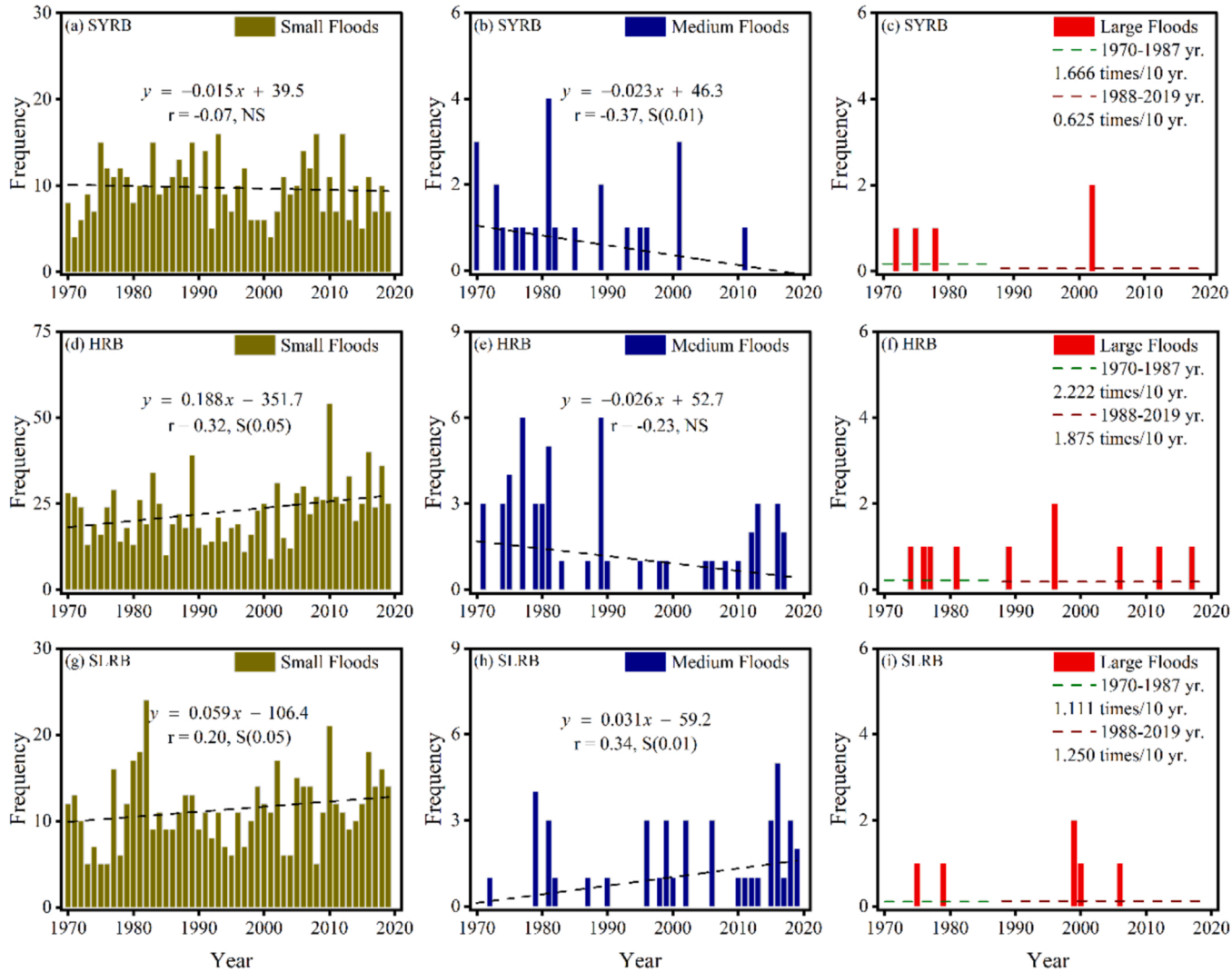


Fig. 6. Trends in flood frequency for the SYRB, HRB, and SLRB in the QM region of northwest China. (a), (d), and (g) Small floods; (b), (e), and (h) medium floods; (c), (f), and (i) large floods. M-K trend tests for the various frequency series detected trends at the 90%, 95%, and 99% significance levels. S means statistically significant at the significance level shown in parentheses; NS means nonsignificant.

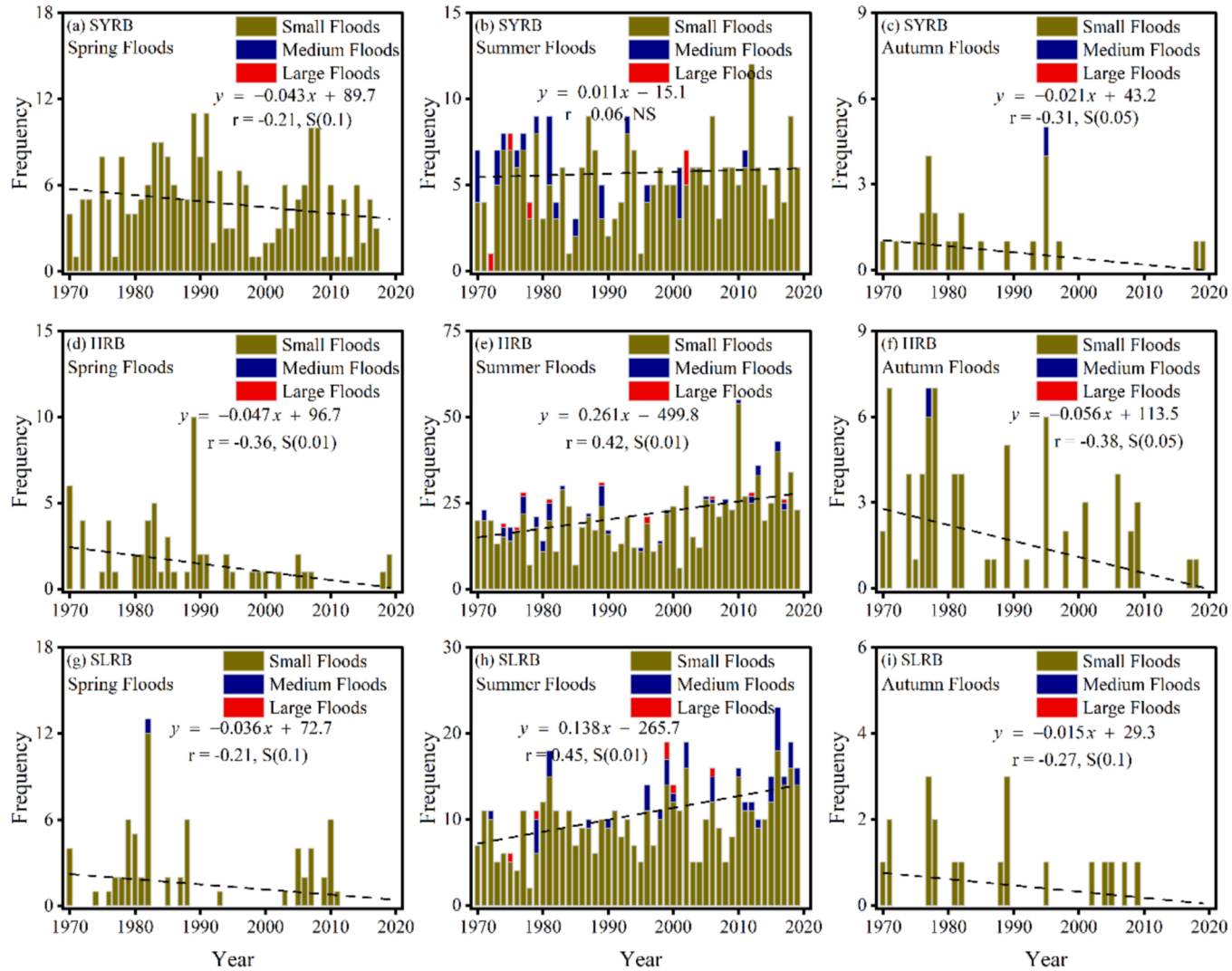


Fig. 7. Trends in flood frequency for various flood types in the SYRB, HRB, and SLRB in the QM region of northwest China. (a), (d), and (g) Spring floods; (b), (e), and (h) summer floods; (c), (f), and (i) autumn floods. M-K trend tests for the various frequency series detected trends at the 90%, 95%, and 99% significance levels. S means statistically significant at the significance level shown in parentheses; NS means nonsignificant.

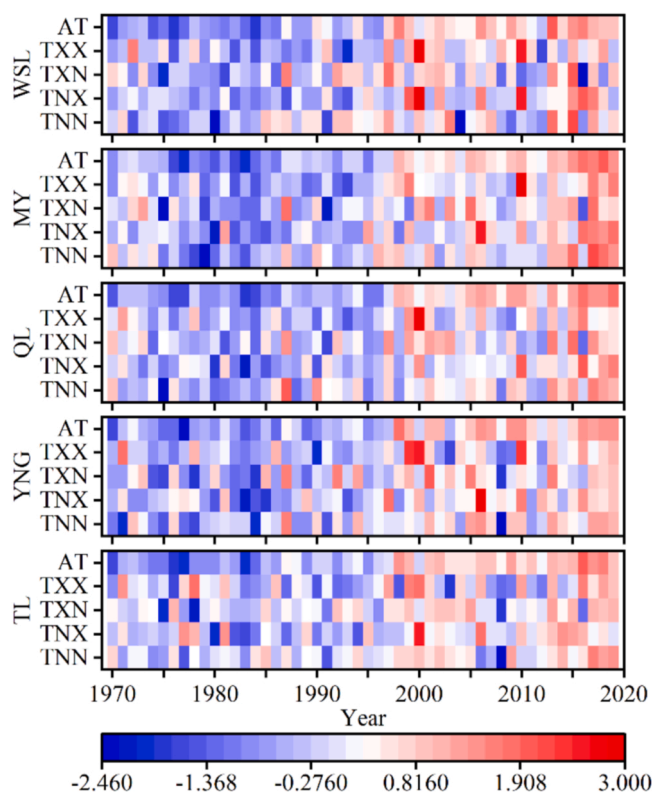


Fig. 8. Temporal variations in temperature indices at meteorological stations in the QM region. The stations are: WSL: Wushaoling; MY: Menyuan; QL: Qilian; YNG: Yeniugou; TL: Tuole. Definitions of the temperature indices are given in Table 3.

slight decrease in the eastern WSL–MY meteorological stations and an increasing trend in the central QL–YNG meteorological stations and western TL meteorological station. Comparing the trends of flood frequency and precipitation (AP, P1 and P5) for the whole region and the three sub-basins (Figs. 3–7, 10), the trends of small and medium floods are generally consistent with the trends of precipitation during the study period, however, large floods are theoretically generated by extreme precipitation, but no obvious correspondence is found in the study area, mainly because the available data from meteorological stations are too few to precisely quantify the process of precipitation and large flood generation. Similar results have been obtained for high-latitude rivers in the Tianshan mountains and the Tarim River basin (Mao et al., 2012; Zhang et al., 2015). Notwithstanding the spatial heterogeneity of the observational records, the changes in flood characteristics identified in our study are broadly consistent with the changing climate. Studies conducted in Europe and North America have shown similar results, such as a changing climate both increasing and decreasing the frequency of European river floods and warmer temperatures leading to earlier spring snowmelt floods (Bloeschl et al., 2019), however, studies conducted in Canada have indicated that there is an increasing trend in flood frequency, with the timescale varying across regions (Zadeh et al., 2020). Studies have indicated that increased precipitation has resulted in increased flooding in some areas, while decreased precipitation and increased evaporation have led to decreased flooding in other areas (Bloeschl et al., 2019; Hodgkins et al., 2017; Zhang et al., 2016). Nevertheless, changes in flood discharge in the context of climate change should be confirmed by a further study based on simulation in high altitude mountainous regions of the QMs because no coherent large-scale gauging dataset has been available, due to the limited spatial coverage and number of meteorological and hydrological stations.

4.2. Differences in trends of different types of floods

Differences were observed between the trends in the frequency of the various flood series of the SYRB, HRB, and SLRB over different time periods, with an important observation being that spring and autumn floods showed decreasing frequency trends and summer floods exhibited increasing frequency trends. Long-term changes in flood frequency highlight the necessity of a better understanding of flood-generation mechanisms in the QM region, which may be obtained through testing the distributions of POT flood series. Flood are classified into seasonable types—i.e., spring, summer, and autumn floods— but these usually occur in high-latitude alpine river areas. Spring floods are induced by snowmelt and occur in late April and May. The April peak in flood frequency in northern China can be attributed to localized storms associated with mid-latitude weather systems in northwest China or to snowmelt in high-altitude regions (Gao et al., 2011; Zhang et al., 2016). Summer floods are caused by heavy rainfall and glacial meltwater (Table 5), and observed mainly in June, July, and August. This rainfall frequently causes annual flood peaks and is the result of the influence of frontal systems or early onset of the East Asian summer monsoon (Ding and Chan, 2005). Autumn floods are triggered by snow and ice melt and rainstorms,

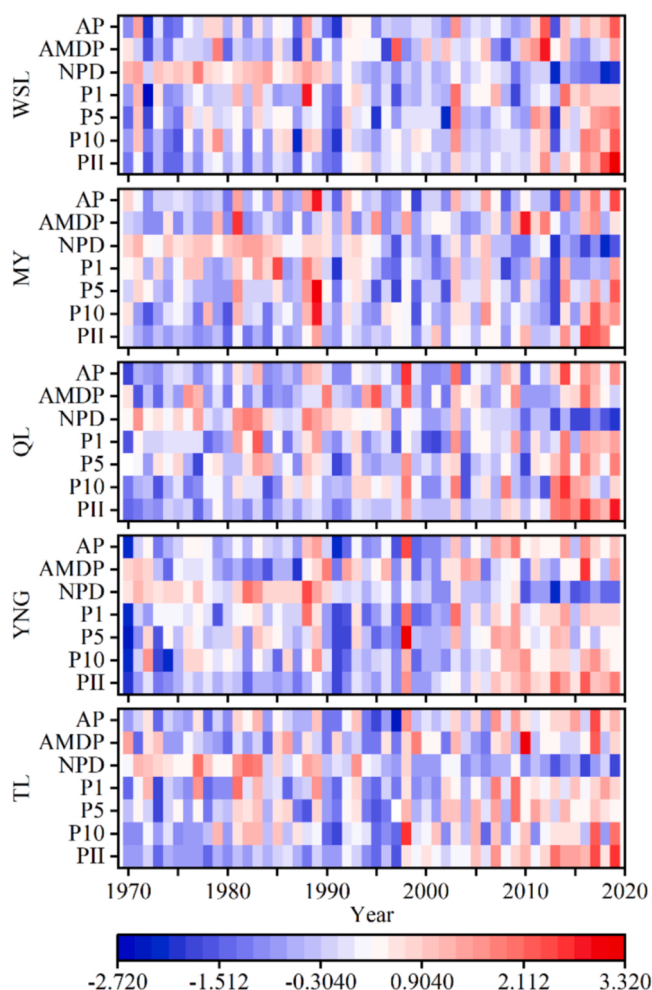


Fig. 9. Temporal variations in precipitation indices at meteorological stations in the QM region. The stations are: WSL: Wushaoling; MY: Menyuan; QL: Qilian; YNG: Yeniugou; TL: Tuole. Definitions of the precipitation indices are given in Table 3.

and generally occur in September. Chen et al. (2015) found that temperature showed an accelerated increase at a rate of 0.517 °C/10 year during 1960–2015 in northwest China, and precipitation was relatively stable from 1960 to 1987 and increased significantly after 1987. Moreover, in the QMs, Wang et al. (2019a) found that spring and autumn precipitation showed a weak increasing trend of 1.85 mm/10 year in 1960–2016, but summer precipitation was significantly increasing at 5.20 mm/10 year, and summer precipitation was the main contributor to the increase in annual precipitation. River floods originating in the QMs can be influenced by many factors, such as altitude, topography, and glacier size, but increased summer precipitation and glacial meltwater due to anomalous warming in the context of climate change are the main reasons for increased summer flooding, while weak changes in precipitation and lower soil moisture due to higher temperatures in spring and autumn are the probable reasons for reduced spring and autumn flooding (Figs. 4 and 7).

4.3. Differences in trends of different regional floods

The spatial distributions of the flood frequency series also differed, with an increasing frequency trend and greater values in the western SLRB and a decreasing frequency trend and smaller values for floods in the SYRB and HRB, as shown in Figs. 3–7. The SYRB in the east is mainly influenced by the East Asian monsoon, the SLRB in the west is mainly influenced by the westerly circulation, while the HRB in the center is the confluence zone, mainly influenced by the Tibetan Plateau monsoon and the above two together, and the enhanced westerly circulation and increased water vapor are the main factors of the increased rainfall in QMs (Chen et al., 2018; Wang et al., 2019a). The different climate types lead to different regional rainfall, which affects the difference of flooding trends between east and west regions. Mountainous areas with greater precipitation and extensive glacier and snow cover have larger floods than plain areas that have lower precipitation and sparser vegetation (Jia et al., 2014; Zhao et al., 2021; Zhu and Wang, 1996). From 2005–2010, 2684 glaciers were present in the QM region, covering an area of $1597.81 \pm 70.30 \text{ km}^2$ with a total ice volume of 84.48 km^3 . Glaciers

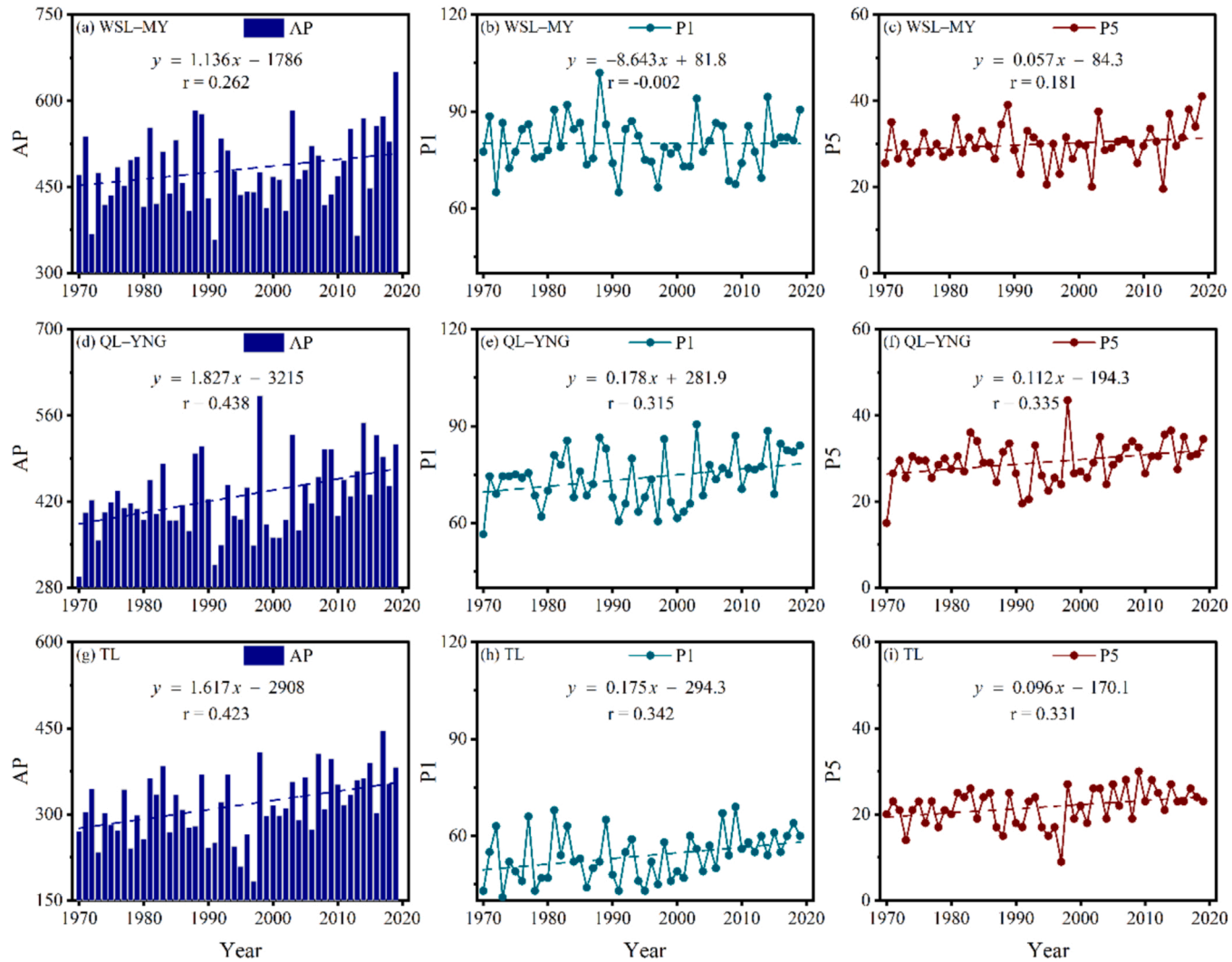


Fig. 10. Temporal variations in precipitation indices at meteorological stations in the QM region. (a), (b), and (c) Mean values for the Wushaoling and Menyuan stations; (d), (e), and (f) Mean values for the Qilian and Yeniugou stations; (g), (h), and (i) Tuole station. Definitions of the temperature and precipitation indices are given in Table 3.

Table 5
Glacier area and percentage of glacier meltwater runoff in this study (Liu et al., 2021).

River Basin	Code	River Name	Glacier area/ to-basin ratio (km ²)/ (%)	Glacial meltwater ratio (%)	Periods
SYRB	1	Gulang	–/ –	–	1960–2010 s
	2	Zamu	3.75/ 0.5	1.3	1960–2010 s
	3	Xiyang	19.77/ 1.8	5.3	1960–2010 s
HRB	4	Babao	–/ –	–	1960–2010 s
	5	Hei	58.90/ 1.2	2.7	1960–2010 s
	6	Dazhuma	5.94/ 2.6	11.4	1960–2010 s
	7	Liyuan	16.28/ 1.5	7.1	1960–2010 s
	8	Hongshui	125.62/ 8.0	44.0	1960–2010 s
	9	Taolai	137.89/ 1.9	17.2	1960–2010 s
SLRB	10	Shiyu	6.38/ 1.0	19.3	1960–2010 s
	11	Shule	469.52/ 4.3	42.2	1960–2010 s
	12	Danghe	233.83/ 1.6	46.8	1960–2010 s

in the east of the region are retreating rapidly, whereas those in central and western areas are retreating more slowly (Wang et al., 2011). Due to differences between the amounts of snow and number of glaciers and glacier area for the 12 rivers in the three main basins in the region, the glacial meltwater runoff recharge rate is < 10% in the SYRB in the east, 5–15% in the HRB in the central region, and > 30% in the SLRB in the west (Table 5) (Gao et al., 2011; Liu et al., 2021; Sun et al., 2018). Significant temperature increases have caused glacial melting and significantly increased precipitation at the QL, YNG, and TL meteorological stations (Figs. 8 and 9), resulting in an increase in flood frequency (Figs. 3–7) and hence the occurrence of extreme floods, especially in the SLRB. In contrast, in SYRB and HRB, the combination of increased temperature and precipitation fluctuations influenced by the westerly circulation, the Tibetan Plateau monsoon and the East Asian monsoon, and the relatively small proportion of glacial meltwater (Table 5) leads to an increasing and decreasing trend in flood frequency. Nevertheless, temperatures and precipitation have increased at different rates in the SYRB, HRB, and SLRB over the past 50 years (Figs. 8 and 9), which is the main reasons for the differences in different levels and types of floods among the eastern and western regions of the QMs (Figs. 6 and 7).

5. Conclusions

The trends in frequency of different flood levels and flood types under the influence of climate change in the QM region of northwest China were investigated using a linear regression estimator and M–K trend tests. The GEV distribution method was adopted to estimate the flood quantiles for different return periods during the historical period, and POT flood series were determined for each river. The timings of floods from 1970 to 2019 were investigated to evaluate trends in flood seasonality under a warming climate. The main conclusions are summarised as follows:

1. POT flood events originating in the QM have complex causes and are affected by various factors. As the temperature and precipitation in arid and semi-arid areas of northwest China showed an increase after 1987, the main factors generating flooding in the QMs are heavy rainfall, abnormal warming, and accelerated glacial melting.
2. Trend analysis for the POT flood series for the 12 studied rivers over the period 1970–2019 identified an increase in the frequency of total floods at the 90% significance level. However, there were differences between the frequency of various flood levels, with an increasing frequency trend for small floods and a decreasing frequency trend for medium and large floods. The spatial distribution of the POT flood series also varied. The overall flood frequency in the SYRB in the east of the region showed a decreasing trend, flood frequency in the HRB in the central part of the region exhibited a significantly increasing trend for small floods but no significant trends for medium or large floods, and flood frequency in the SLRB in the west of the region showed significantly increasing trends for small and medium floods but a nonsignificant trend for large floods.
3. The 12 rivers analysed in this study all originate from glaciers in the QM region, and their upstream areas are pristine and unaffected by human activities. According to our data analysis, spring and autumn floods showed decreasing frequency trends and summer floods exhibited increasing frequency trends in the SYRB, HRB, and SLRB.

In the future, research on the formation mechanism of extreme flood events should be strengthened, especially to identify the impact of climate change and human activities. The findings can propose more targeted adaptation to climate change recommendations and countermeasures.

CRedit authorship contribution statement

Xueliang Wang: Writing – original draft preparation, Conceptualization, Methodology, Software, Writing – review & editing. **Rensheng Chen:** Resources, Funding Acquisition, Supervision, Data curation. **Hongyuan Li:** Visualization, Investigation. **Kailu Li:** Visualization. **Junfeng Liu:** Formal analysis. **Guohua Liu:** Data curation.

Declaration of Competing Interest

The authors declare that they have no known competing financial interests or personal relationships that could have appeared to influence the work reported in this paper.

Data availability statement

Meteorological data are collected by the National Climate Center of the China Meteorological Administration and available on <http://data.cma.cn/> under request. Flood data are collected by Bureau of Hydrology and Water Resources of Gansu Province, China, and available under request.

Acknowledgments

This study was supported by the National Key Research and Development Program of China (2019YFC1510505), the National Natural Science Foundation of China (42171145), the Joint Research Project of Three-River Headwaters National Park, Chinese Academy of Sciences and the People's Government of Qinghai Province (LHZX-2020-11), the Natural Science Foundation of Gansu Province, China (21JR7RA043), the Qinghai Key R&D and Transformation Program (2020-SF-146), and the Open Research Fund of the National Cryosphere Desert Data Center (2021kf09).

Appendix A. Supporting information

Supplementary data associated with this article can be found in the online version at [doi:10.1016/j.ejrh.2022.101153](https://doi.org/10.1016/j.ejrh.2022.101153). These data include Google maps of the most important areas described in this article.

References

- Archfield, S., Hirsch, R., Viglione, A. and Blöschl, G., 2014. Using a peaks-over-threshold approach to assess changes in flood magnitude, volume, duration, and frequency across the United States, Egu General Assembly Conference.
- Betts, R.A., 2011. The science of climate change, 1261-1261 Science 292 (5520). <https://doi.org/10.1002/9781118266748.ch1>.
- Bloeschl, G., et al., 2019. Changing climate both increases and decreases European river floods (+). Nature 573 (7772), 108. <https://doi.org/10.1038/s41586-019-1495-6>.
- Bloeschl, G., et al., 2017. Changing climate shifts timing of European floods. Science 357 (6351), 588–590. <https://doi.org/10.1126/science.aan2506>.
- Cao, B., et al., 2014. Changes in the glacier extent and surface elevation along the Ningchan and Shuiguan river source, eastern Qilian Mountains, China. Quatern. Res. 81 (3), 531–537. <https://doi.org/10.1016/j.yqres.2014.01.011>.
- Chen, R., et al., 2021. Progress and issues on key technologies in forecasting of snowmelt flood disaster in arid areas, Northwest China. Adv. Earth Sci. 36 (3), 233–244.
- Chen, R.S., et al., 2018. Maximum precipitation altitude on the northern flank of the Qilian Mountains, northwest China. Hydrol. Res. 49 (5), 1696–1710. <https://doi.org/10.2166/nh.2018.121>.
- Chen, Y.N., Li, Z., Fan, Y.T., Wang, H.J., Deng, H.J., 2015. Progress and prospects of climate change impacts on hydrology in the arid region of northwest China. Environ. Res. 139, 11–19. <https://doi.org/10.1016/j.envres.2014.12.029>.
- Desai, B., Maskrey, A., Peduzzi, P., De Bono, A. and Herold, C., 2015. Making Development Sustainable: The Future of Disaster Risk Management, Global Assessment Report on Disaster Risk Reduction.
- Ding, Y.H., Chan, J.C.L., 2005. The East Asian summer monsoon: an overview. Meteorol. Atmos. Phys. 89 (1–4), 117–142. <https://doi.org/10.1007/s00703-005-0125-z>.
- Durocher, M., Zadeh, S.M., Burn, D.H., Ashkar, F., 2018. Comparison of automatic procedures for selecting flood peaks over threshold based on goodness-of-fit tests. Hydrol. Process. 32 (18), 2874–2887. <https://doi.org/10.1002/hyp.13223>.
- Gao, X., Zhang, S.Q., Ye, B.S., Gao, H.K., 2011. Recent changes of glacier runoff in the Hexi Inland river basin. Adv. Water Sci. 22 (3), 344–350.
- Gocic, M., Trajkovic, S., 2013. Analysis of changes in meteorological variables using Mann-Kendall and Sen's slope estimator statistical tests in Serbia. Glob. Planet. Change 100, 172–182. <https://doi.org/10.1016/j.gloplacha.2012.10.014>.
- Gu, L., et al., 2021. On future flood magnitudes and estimation uncertainty across 151 catchments in mainland China. Int. J. Climatol. 41, E779–E800. <https://doi.org/10.1002/joc.6725>.
- Hallegrate, S., Green, C., Nicholls, R.J., Corfee-Morlot, J., 2013. Future flood losses in major coastal cities. Nat. Clim. Chang. 3 (9), 802–806. <https://doi.org/10.1038/nclimate1979>.
- Hamed, K.H., 2008. Trend detection in hydrologic data: the Mann-Kendall trend test under the scaling hypothesis. J. Hydrol. 349 (3–4), 350–363. <https://doi.org/10.1016/j.jhydrol.2007.11.009>.
- Hirabayashi, Y., et al., 2013. Global flood risk under climate change. Nat. Clim. Chang. 3 (9), 816–821. <https://doi.org/10.1038/nclimate1911>.
- Hodgkins, G.A., et al., 2017. Climate-driven variability in the occurrence of major floods across North America and Europe. J. Hydrol. 552, 704–717. <https://doi.org/10.1016/j.jhydrol.2017.07.027>.
- IPCC, 2021. Intergovernmental Panel on Climate Change, Climate Change 2021: Impacts, Adaptation, and Vulnerability. Cambridge Univ.Press, Cambridge, U. K.
- Jia, W., Zhang, Y., Li, Z., 2014. Spatial and temporal change of precipitation extremes in Qilian Mountains and Hexi Corridor in recent fifty years. Sci. Geogr. Sin. 34 (8), 1002–1009.
- Jiang, J.X., Cai, M., Xu, Y.J., Fang, G.H., 2021. The changing trend of flooding in the Aksu River basin. J. Glaciol. Geocryol. 43 (1), 1–10.
- Katz, R.W., Parlange, M.B., Naveau, P., 2002. Statistics of extremes in hydrology. Adv. Water Resour. 25 (8), 1287–1304. [https://doi.org/10.1016/S0309-1708\(02\)00056-8](https://doi.org/10.1016/S0309-1708(02)00056-8).
- Kendall, M.G., 1975. Rank correlation methods. Brit. J. Psychol. 25 (1), 86–91. <https://doi.org/10.1111/j.2044-8295.1934.tb00727.x>.
- Kundzewicz, Z.W., et al., 2019a. Flood risk in a range of spatial perspectives – from global to local scales. Nat. Hazard. Earth Sys. 19 (7), 1319–1328. <https://doi.org/10.5194/nhess-19-1319-2019>.
- Kundzewicz, Z.W., et al., 2019b. Flood risk and its reduction in China. Adv. Water Resour. 130, 37–45. <https://doi.org/10.1016/j.advwatres.2019.05.020>.

- Lang, M., Ouarda, T., Bobee, B., 1999. Towards operational guidelines for over-threshold modeling. *J. Hydrol.* 225 (3–4), 103–117. [https://doi.org/10.1016/S0022-1694\(99\)00167-5](https://doi.org/10.1016/S0022-1694(99)00167-5).
- Li, Z., Li, Q., Wang, J., Feng, Y., Shao, Q., 2020. Impacts of projected climate change on runoff in upper reach of Heihe River basin using climate elasticity method and GCMs. *Sci. Total Environ.* 716, 137072. <https://doi.org/10.1016/j.scitotenv.2020.137072>.
- Li, Z.L., Xu, Z.X., Li, J.Y., Li, Z.J., 2008. Shift trend and step changes for runoff time series in the Shiyang River basin, northwest China. *Hydro. Process* 22 (23), 4639–4646. <https://doi.org/10.1002/hyp.7127>.
- Liang, C., et al., 2019. Assessing urban flood and drought risks under climate change, China. *Hydrol. Process.* 33 (9), 1349–1361. <https://doi.org/10.1002/hyp.13405>.
- Liu, G.H., Chen, R.S., Li, K.L., 2021. Glacial change and its hydrological response in three inland river basins in the Qilian Mountains, western China. *Water* 13 (16). <https://doi.org/10.3390/w13162213>.
- Ma, Z.M., Kang, S.Z., Zhang, L., Tong, L., Su, X.L., 2008. Analysis of impacts of climate variability and human activity on streamflow for a river basin in arid region of northwest China. *J. Hydrol.* 352 (3–4), 239–249. <https://doi.org/10.1016/j.jhydrol.2007.12.022>.
- Mann, H.B., 1945. Nonparametric test against trend. *Econometrica* 13 (3), 245–259. <https://doi.org/10.2307/1907187>.
- Mao, W., et al., 2012. Variations of extreme flood of the Rivers in Xinjiang Region and Some Typical Watersheds from Tianshan Mountains and their response to climate change in recent 50 years. *J. Glaciol. Geocryol.* 34 (5), 1037–1046.
- Milly, P.C.D., Wetherald, R.T., Dunne, K.A., Delworth, T.L., 2002. Increasing risk of great floods in a changing climate. *Nature* 415 (6871), 514–517. <https://doi.org/10.1038/415514a>.
- Murray, V., Ebi, K.L., 2012. IPCC special report on managing the risks of extreme events and disasters to advance climate change adaptation (SREX). *J. Epidemiol. Community Health* 66 (9), 759–760. <https://doi.org/10.1136/jech-2012-201045>.
- Sang, Y.F., Wang, Z., Liu, C., 2014. Comparison of the MK test and EMD method for trend identification in hydrological time series. *J. Hydrol.* 510, 293–298. <https://doi.org/10.1016/j.jhydrol.2013.12.039>.
- Shao, Q.X., Wong, H., Xia, J., Ip, W.C., 2004. Models for extremes using the extended three-parameter Burr XII system with application to flood frequency analysis. *Hydrol. Sci. J. - J. Sci. Hydrol.* 49 (4), 685–702. <https://doi.org/10.1623/hysj.49.4.685.54425>.
- Shi, Y., et al., 2003. Discussion on the present climate change from warm-dry to warm-wet in northwest china. *Quatern. Sci.* 23 (2), 152–164.
- Smith, J.A., Cox, A.A., Baeck, M.L., Yang, L., Bates, P., 2018. Strange floods: the upper tail of flood peaks in the United States. *Water Resour. Res.* 54 (9), 6510–6542. <https://doi.org/10.1029/2018wr022539>.
- Sun, M.P., Liu, S.Y., Yao, X.J., Guo, W.Q., Xu, J.L., 2018. Glacier changes in the Qilian Mountains in the past half-century: based on the revised first and second Chinese glacier inventory. *J. Geogr. Sci.* 28 (2), 206–220. <https://doi.org/10.1007/s11442-018-1468-y>.
- Tian, H., Yang, T., Liu, Q., 2014. Climate change and glacier area shrinkage in the Qilian mountains, China, from 1956 to 2010. *Ann. Glaciol.* 55 (66), 187–197. <https://doi.org/10.3189/2014AoG66A045>.
- Wang, L., et al., 2019a. Change characteristics of precipitation and temperature in the Qilian Mountains and Hexi Oasis, Northwestern China. *Environ. Earth Sci.* 78 (9), 13. <https://doi.org/10.1007/s12665-019-8289-x>.
- Wang, P., Li, Z.Q., Gao, W.Y., 2011. Rapid shrinking of glaciers in the middle qilian mountain region of northwest China during the last similar to 50 years. *J. Earth Sci.* 22 (4), 539–548. <https://doi.org/10.1007/s12583-011-0195-4>.
- Wang, X., et al., 2019b. Changes in river discharge in typical mountain permafrost catchments, northwestern China. *Quatern. Int.* 519, 32–41. <https://doi.org/10.1016/j.quaint.2018.11.010>.
- Wang, Y., Qin, D., 2017. Influence of climate change and human activity on water resources in arid region of Northwest China: an overview. *Clim. Chang. Res.* 13 (5), 483–493.
- Wilby, R.L., Keenan, R., 2012. Adapting to flood risk under climate change. *Prog. Phys. Geogr.* 36 (3), 348–378. <https://doi.org/10.1177/0309133312438908>.
- Xiong, B., et al., 2020. Nonstationary frequency analysis of censored data: a case study of the floods in the Yangtze River from 1470 to 2017. *Water Resour. Res.* 56 (8), 20. <https://doi.org/10.1029/2020wr027112>.
- Yang, L., Wang, L.C., Li, X., Gao, J., 2019. On the flood peak distributions over China. *Hydrol. Earth Syst. Sci.* 23 (12), 5133–5149. <https://doi.org/10.5194/hess-23-5133-2019>.
- Yang, Y., Chen, R.S., Liu, G.H., Liu, Z.W., Wang, X.Q., 2022. Trends and variability in snowmelt in China under climate change. *Hydrol. Earth Syst. Sci.* 26 (2), 305–329. <https://doi.org/10.5194/hess-26-305-2022>.
- Yin, J., Ye, M.W., Yin, Z., Xu, S.Y., 2015. A review of advances in urban flood risk analysis over China. *Stoch. Environ. Res. Risk Assess.* 29 (3), 1063–1070. <https://doi.org/10.1007/s00477-014-0939-7>.
- Zadeh, S.M., Burn, D.H., O'Brien, N., 2020. Detection of trends in flood magnitude and frequency in Canada. *J. Hydrol. -Reg. Stud.* 28, 13. <https://doi.org/10.1016/j.ejrh.2020.100673>.
- Zhang, Q., et al., 2016. Magnitude, frequency and timing of floods in the Tarim River basin, China: changes, causes and implications. *Glob. Planet. Change* 139, 44–55. <https://doi.org/10.1016/j.gloplacha.2015.10.005>.
- Zhang, Q., Li, J.F., Singh, V.P., Xiao, M.Z., 2013. Spatio-temporal relations between temperature and precipitation regimes: Implications for temperature-induced changes in the hydrological cycle. *Glob. Planet. Change* 111, 57–76. <https://doi.org/10.1016/j.gloplacha.2013.08.012>.
- Zhang, Q., Yu, Y.X., Zhang, J., 2008. Characteristics of water cycle in the Qilian Mountains and the Oases in Hexi Inland River Basins. *J. Glaciol. Geocryol.* 30 (6), 907–913.
- Zhang, Y., Liu, S., Shangguan, D., Li, J., Zhao, J., 2012. Thinning and shrinkage of Laohugou No. 12 glacier in the Western Qilian Mountains, China, from 1957 to 2007. *J. Mt. Sci.* 9 (3), 343–350. <https://doi.org/10.1007/s11629-009-2296-4>.
- Zhang, Y.Y., Fu, G.B., Sun, B.Y., Zhang, S.F., Men, B.H., 2015. Simulation and classification of the impacts of projected climate change on flow regimes in the arid Hexi Corridor of Northwest China. *J. Geophys. Res. -Atmos.* 120 (15), 7429–7453. <https://doi.org/10.1002/2015jd023294>.
- Zhao, C.C., Ding, Y.J., Yao, S.X., 2021. The variation of precipitation and rain days for different intensity classes during the rainy season in the Qilian Mountains, Northwest China. *Theor. Appl. Climatol.* 144 (1–2), 163–178. <https://doi.org/10.1007/s00704-020-03514-8>.
- Zhu, S.S., Wang, Q., 1996. Temporal-spatial distributions and recent changes of precipitation in the Northern Slopes of the Qilian mountains. *J. Glaciol. Geocryol.* 18, 296–304.
- Ziegler, A.D., et al., 2003. Detection of intensification in global- and continental-scale hydrological cycles: temporal scale of evaluation. *J. Clim.* 16 (3), 535–547. [https://doi.org/10.1175/1520-0442\(2003\)016#0535:iga\\$2.0.Co;2](https://doi.org/10.1175/1520-0442(2003)016#0535:iga$2.0.Co;2).